IEEE Access
Multidisciplinary | Rapid Review | Open Access Journal

Received 15 November 2023, accepted 30 November 2023, date of publication 12 December 2023,
date of current version 20 December 2023.

Digital Object Identifier 10.1109/ACCESS.2023.3341623

RESEARCH ARTICLE

Impact of Beamforming Algorithms on the Actual RF EMF Exposure From Massive MIMO Base Stations

MARCIN RYBAKOWSKI[1,3], KAMIL BECHTA[1], CHRISTOPHE GRANGEAT[2], AND PAWEL KABACIK[3]

[1]Mobile Networks, Nokia, 54-155 Wroclaw, Poland
[2]Mobile Networks, Nokia, 11351 Paris, France
[3]Faculty of Electronics, Photonics and Microsystems, Wroclaw University of Science and Technology, 50-370 Wroclaw, Poland

Corresponding author: Marcin Rybakowski (marcin.rybakowski@nokia.com)

This work was supported in part by Nokia through EU under Grant POIR.01.01.01-00-0008/21, and in part by the "Industry Ph.D." Program (Doktorat Wdrożeniowy) of the Polish Ministry of Science and Higher Education.

ABSTRACT Base stations equipped with large multi-antenna systems and associated beamforming schemes provide large capacity and coverage. Massive multiple-input-multiple-output (MIMO) with beamforming was introduced as one of the enablers of 5G system performance, and this technology is evolving with the introduction of more advanced algorithms for spatial multiplexing. One of the most relevant conditions to support deployment of 5G base stations with massive MIMO is to assess realistic RF electromagnetic field exposure compliance distances leveraging the actual maximum approach introduced in IEC 62232:2022. This evaluation method takes into account the variability of traffic load and beam patterns used by the beamforming algorithm. This work investigates the impact of various beamforming schemes, like grid-of-beams, eigen-beamforming and zero-forcing, as well as various array antenna configurations on the evaluation of the power reduction factor used when implementing the actual maximum approach for RF electromagnetic field compliance assessment of massive MIMO base stations. The modelling results show that lower power reduction factors can be considered for eigen-beamforming and zero-forcing beamforming algorithms compared to grid-of-beam. The power reduction factor drop can be up to −4 dB when 8 user equipment's are connected simultaneously.

INDEX TERMS 5G, actual maximum approach, antenna array, beamforming, Eigen-beamforming, grid-of-beams beamforming, EMF exposure, multi-antenna system, zero-forcing beamforming.

I. INTRODUCTION

The 5th generation (5G) of mobile communication systems is being deployed around the world. Many of the new base stations (BS) are operating in the 3.5 GHz band and are equipped with multi-antenna systems with massive multiple-input-multiple-output (MIMO) technology [1]. Multi-antenna systems with associated beamforming (BF) algorithms increase capacity and coverage of the cell in comparison to the previous mobile networks equipped with sectoral antennas. The overall performance of the network strongly depends on the BF algorithms embedded in the BS multi-antenna system.

The first deployment of 5G BS is mainly based on the simple grid-of-beams (GoB) algorithm, where beams steered towards the user equipment (UE) location are selected from a predefined set. However, more advanced BF schemes have been adopted to meet the expected requirements of the 5G system. One of the well-known BF algorithms is eigen-beamforming (EBF), which provides much better resolution in terms of beam steering directions than GoB and can adapt to changing radio propagation conditions. Another BF scheme is eigen-mode zero-forcing (EZF), which minimizes interference towards non-served UEs by null-forming in beam pattern. Both EBF and EZF algorithms are very effective and provide much better performance than GoB, but on the other hand require higher signal processing

The associate editor coordinating the review of this manuscript and approving it for publication was Yuan Gao.

capacity inside the base-band modules of massive MIMO BS [1].

An important condition to support the deployment of massive MIMO BS is to provide an accurate and realistic assessment of RF electromagnetic field (EMF) exposure using the averaging time specified in the applicable exposure limits, such as [2], [3] or [4]. The high dynamics of BF require to develop a new method for evaluation of RF EMF exposure from multi-antenna system [5]. The traditional approach based on the configured maximum equivalent-isotropic-radiated-power (EIRP) may lead to large overestimation of the compliance distances around the BS. The actual maximum approach, as specified in IEC 62232:2022 [5], takes into account the variability of the traffic load and the beam patterns used during BF operations in the evaluation of compliance distances. Examples of statistical analysis of RF exposure on operational networks are provided in IEC TR 62669:2019 [6] including both measurement and modelling methods. Many publications analyzed the actual maximum approach for massive MIMO systems using one selected BF method without comparison to other schemes, e.g., [7], [8], [9], and [10]. The impact of BF algorithms on RF EMF exposure was studied in [11], however with only one specific deployment of a single BS and with a ray-tracing channel model. In this work we expand the statistical analysis presented in [7] to various additional BF techniques and massive MIMO antenna configurations to support the implementation of the actual maximum approach for RF EMF exposure evaluation. We focus only on time division duplex (TDD) mode because massive MIMO is deployed mainly on TDD frequency bands, but the main conclusions and observations would remain the same for frequency division duplex (FDD). We use advanced system-level simulation with 3D statistical spatial modeling of radio propagation and different distribution of UEs as in the previous study [7], which allows us to provide comprehensive insight into this topic. This paper has been divided into the following parts: Section II explains the basics of analyzed BF algorithms, Section III describes the simulation methodology in details, Sections IV compares performance results of 5G system operating with three different BF schemes, Sections V focuses on EMF exposure analysis in accordance with the actual maximum approach, whereas Section VI concludes the study and provides further research topics in this subject area.

II. THE BASICS OF BEAMFORMING ALGORITHMS

The main benefits of multi-antenna systems regarding cell coverage and capacity come from two complementary techniques: BF and spatial multiplexing, as shown in Figure 1. When using BF, the BS directs the transmitted energy towards a specific UE, which greatly increases the power of the received signal but also minimizes transmission of energy in other directions. This avoids unnecessary power consumption and reduces RF EMF exposure where there is no user. In spatial multiplexing, the BS sends multiple streams to

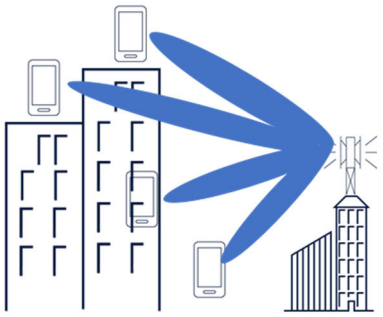

FIGURE 1. Illustration of massive MIMO principles: spatial (angular) separation of UEs to provide multiplexing gain on orthogonal beams.

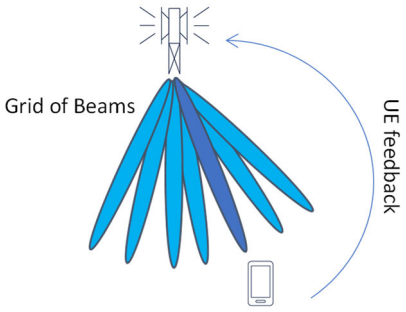

FIGURE 2. Illustration of UE-feedback-based BF with GoB.

several spatially separated UEs using an BF algorithm, which additionally increases the spectral efficiency.

The key enabler of BF is channel estimation, where two main approaches can be distinguished. The first approach is based on UE feedback, where the UE measures downlink (DL) reference signals transmitted by the BS, identifies the best beam from the set of predefined beams (e.g. GoB) and indicates this to the BS (Figure 2). Due to the robustness of this technique, it can work under any radio channel conditions. However, beam selection may be suboptimal due to insufficient channel information and low resolution of beams. The second approach relies on the radio channel reciprocity, where the properties of the DL channel can be estimated using uplink (UL) channel measurements. The BS measures the UL Sounding Reference Signal (UL SRS) sent by the UE, processes the received information, estimates the DL channel, and selects or creates the optimal beam (Figure 3). This technique allows optimal beam selection and BF weights adaptation due to more accurate channel estimation. Reciprocity-based channel estimation also allows to adapt beams shapes to minimize interference, e.g., by the EZF approach as presented in Figure 4. Theoretically, an unlimited number of beams can be constructed using reciprocity-based techniques. However, this technique requires high quality channel estimation and sufficient UL link budget due to the limited transmit power of UE. Therefore, the cell coverage range in which reciprocity-based channel estimation can be used is limited.

The EBF and EZF techniques exploit multipath propagations, so that UE-specific beams can be constructed into several other directions, apart from the main lobes. The resulting

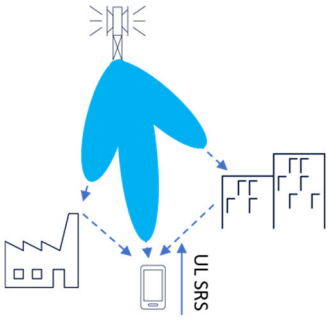

FIGURE 3. Illustration of reciprocity-based EBF.

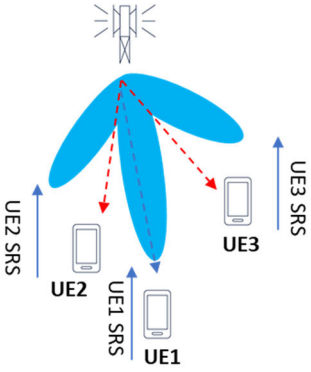

FIGURE 4. Illustration of reciprocity-based EZF.

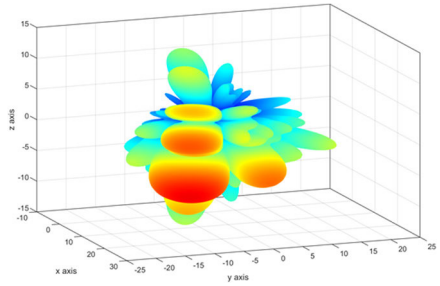

FIGURE 5. Illustration of resulting 3D beam pattern of EBF algorithm for one example of radio channel realization.

beam may have an arbitrary shape where multiple beams cover several propagation paths, as shown in Figure 5.

Small scale fading effects in realistic multi-path channels with angular spread impact the effective beam shape, which is highly phase dependent, as described, for example, in [12]. Therefore, it is interesting to study the effect of these highly dynamic and unpredictable beam shapes on the exposure to RF EMF, especially in the context of the estimation of power reduction factor (F_{PR}) used in the actual maximum approach for massive MIMO BS as described in IEC 62232: 2022 [5].

III. SIMULATION METHODOLOGY

Computational modeling is listed in IEC 62232:2022 [5] and IEC TR 62669:2019 [6], next to the measurement methods, as one of the recommended approaches for analyzing the

FIGURE 6. Antenna array with 8 × 8 cross-polarized antenna elements formed in 16 sub-arrays. Each sub-array is connected to 2 TRX (1 TRX per polarization).

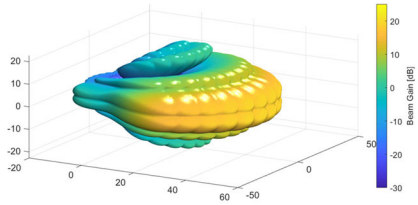

FIGURE 7. 3D envelope of antenna beam patterns for GoB.

actual maximum approach and estimate of F_{PR}. Therefore, in this study we used advanced proprietary system-level simulator for massive MIMO networks evaluation. Core of the simulator is based on the statistical 3D spatial model of urban macro (UMa) radio wave propagation in accordance with 3GPP technical report 38.901 [13]. This standardized channel model is commonly used by the industry to build link level and system level simulators. The implementation used in this study has been also used during study described in more details in [7]. All statistical distributions of simulated parameters presented in this paper, e.g., spatial distribution of UEs, are in accordance with this model.

The study was performed for a cellular network consisting of 7 cells, each of cell having 3 sectors with massive MIMO multi-antenna BS operating in time-division-duplex (TDD) scheme with a technology duty-cycle factor of 0.75 for DL. In the scenario, the BS is placed at the height of 25 m with the inter-site distance of 500 m. The system operates at the frequency of 3.5 GHz with 100 MHz channel bandwidth, sub-carrier spacing of 30 kHz and 51 dBm of maximum transmit power. Simulations were conducted for 8 × 8 antenna array with cross-polarized antenna elements and 32 transceivers (TRX) connected to subarrays as depicted in the Figure 6 or 128 TRX connected to all antenna elements. The maximum gain of this antenna array is 23.2 dBi at boresight. The antenna was also configured with 5 ° of electrical down-tilt because UEs are located below the antenna height. Wideband proportional fair scheduler with multi user (MU) MIMO beam pairing based on correlation between beams are used. In the antenna array model, we implemented three different BF algorithms: GoB, EBF and EZF.

In the case of GoB, the antenna array can generate 24 beams per polarization (48 in total) uniformly distributed within 120 degrees of azimuth opening angle and 2 elevation

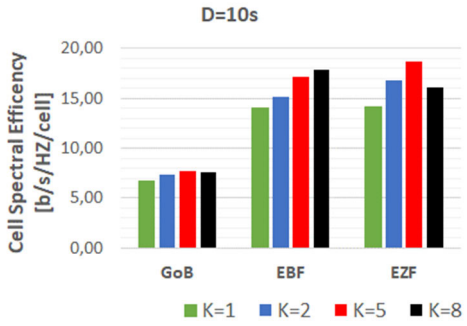

FIGURE 8. Cell spectral efficiency for different BF schemes (32TRX).

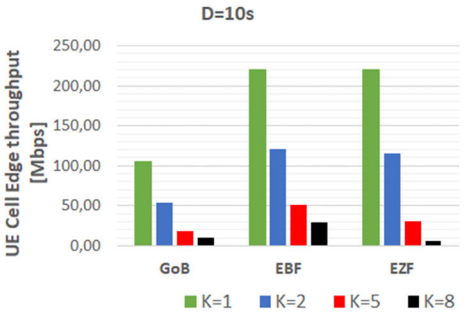

FIGURE 9. UE cell edge throughput for different BF schemes(32 TRX).

angles as shown in Figure 7. A multi-antenna system with GoB can serve many users simultaneously thanks to spatial multiplexing by using different antenna beams with the lowest inter-beam interference but due to limited resolution of beams the MU-MIMO gains are low (see Section IV). In the case of EBF the channel covariance matrix is averaged over the full carrier bandwidth. The strongest eigenvectors (one or several, depending on the rank) of this covariance matrix are used as a precoder. When EZF is used in the simulation model, the channel covariance matrix is also averaged over the full carrier bandwidth. Then, the matrix of strongest eigenvectors (depending on the wanted rank) are used for zero forcing precoding calculation. We do not use pilot contamination in simulation, so Channel State Information (CSI) based on the UL pilot is ideal.

The simulated UEs use a single omnidirectional antenna and are randomly distributed in a cell, where 20% of them are outdoors and 80% indoor, inside the buildings whose heights are uniformly distributed between 4 and 8 floors (model according to 3GPP 38.901 [13]). UEs locations are static but UE positions are randomly rotated every drop. The number of served terminals, K, is 1, 2, 5 or 8 and the drop duration of a single DL connection, D is 10, 60 or 360 s. The averaging time used is 6 minutes as specified in ICNIRP-1998 [2] and IEEE C95.1 [3]. We consider a configuration where the BS are fully loaded using the full-buffer traffic model [7]. Average values of beamforming gain are calculated for every BS and for every subframe to evaluate antenna gain distribution and evaluation of F_{PR}. Table 1 summarizes the main simulation assumptions.

TABLE 1. Main simulation assumptions.

Parameter	*Value*
Channel model	3GPP 38.901 urban macro (UMa)
Carrier frequency	3.5 GHz
Channel bandwidth	100 MHz
Sub-carrier spacing	30 kHz
Max total Tx power of BS (without losses)	51 dBm
No. of TRx	32 or 128
Gain of BS single antenna element	5.2 dBi
Configuration of BS antenna array per polarization	8×8
Electrical down-tilt of BS antenna pattern	5°
TDD duty cycle for DL	0.75
Height of BS antenna array centre	25 m
No. of cells / No. of sectors	7 / 21
Inter-site distance	500 m
Type of UE antenna	Omnidirectional
SU-MIMO maximum rank	2
UE distribution	80% indoor, uniform distribution between 4 to 8 floors
No. of simultaneously served UEs	1, 2, 5 and 8
UE serving time	10 s, 60 s and 360 s
The actual max approach averaging time	6 min

IV. ANALYSIS OF 5G SYSTEM PERFORMANCE WITH DIFFERENT BF ALGORITHMS

Performance comparison of analyzed BF methods with 32 TRX configuration are shown on Figures 8 for spectral efficiency and Figure 9 for cell edge throughput. We observe that EBF and EZF beamforming schemes have higher performance compared to GoB for almost all K and D combinations. The spectral efficiency of GoB is increasing only slightly with more UEs served, which means that performance of MU-MIMO is limited due to a limited number of occasions for MU-MIMO beams pairing due to beam shape and inter-beam interferences. Therefore, with higher number of simultaneously served UEs the scheduler has more difficulty with selecting for example 5 or 8 beams with a sufficiently high signal to interference and noise ratio (SINR). It could be improved by additional side lobe attenuation. This challenge is improved when EBF is implemented in the system. EBF has much higher resolution of antenna beams, which improves MU-MIMO pairing capability. In the case of EZF, the performance for scenarios with 2 and 5 UEs has an improved spectral efficiency compared to EBF due zero-forcing capability, which can cancel interference. This changes, when 8 UEs are simultaneously served and leading to spectral efficiency drop due to the low performance of EZF for cell edge UEs. As seen in Figure 9, the cell edge throughput for EZF with 8 UEs is much lower than for EBF or

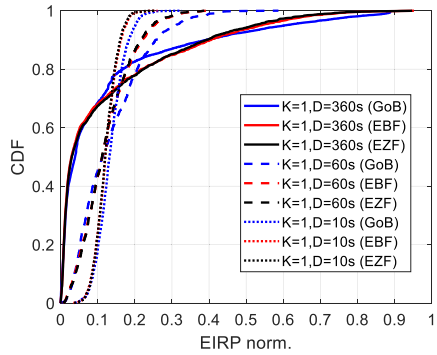

FIGURE 10. CDF of normalized EIRP for different BF schemes and K = 1.

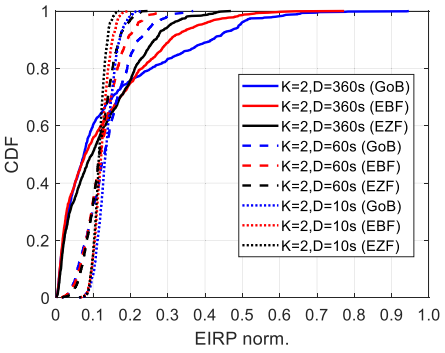

FIGURE 11. CDF of normalized EIRP for different BF schemes and K = 2.

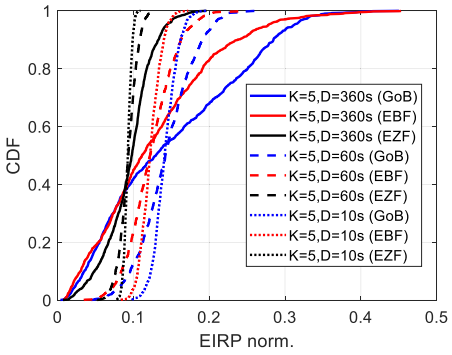

FIGURE 12. CDF of normalized EIRP for different BF schemes and K = 5.

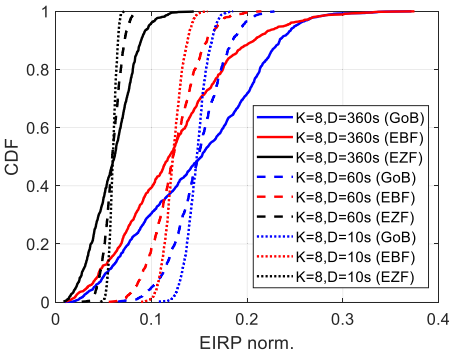

FIGURE 13. CDF of normalized EIRP for different BF schemes and K = 8.

even GoB, because EZF does not prioritize the received signal level, but only co-channel interference. More layers result in a loss of freedom for nulling and large amplitude fluctuations and a relatively low overall transmitted power. Therefore, the cell edge UEs suffer due to the reduced RX signal level and the resulting low SINR due to neighbor cell interference, which is also higher. The higher the number of co-scheduled UEs, the more difficult it is to still get a sufficient level of received DL signal. The BS antenna architecture assumed for simulation is also not optimal for the EZF algorithm with a large number of simultaneously served UEs. This is due to sub-paneling which is reducing the degrees of freedom of EZF for efficient null-forming in elevation.

V. ANALYSIS OF BF ALGORITHM AND ANTENNA ARRAY CONFIGURATION IMPACT ON THE ACTUAL RF EMF EXPOSURE

The simulation results of the actual RF EMF exposure are shown in the form of a cumulative distribution function (CDF) of the averaged EIRP normalized to the maximum EIRP corresponding to the direction of the highest RF EMF exposure.

A. IMPACT OF BF ALGORITHM

The results presented in Figures 10 to Figure 13 correspond to different numbers of served UE, $K = 1$, $K = 2$, $K = 5$ and $K = 8$, respectively, and all assumed values of service time D, obtained for an antenna array with 32 TRX. We observe that the actual RF EMF exposure is reduced with EBF and EZF as compared to that with GoB, which is an expected effect due to the higher dynamic of beam shaping, resulting in reduced actual RF EMF exposure. In the case of one served UE only ($K = 1$) for long time, which is a very rare case in operational networks, the actual RF EMF exposure is also reduced for EBF and EZF compared to GoB. It can be also noticed that results for EBF and EZF are almost the same in the case of $K = 1$, since, for single UE in the cell, there is no need to cancel the interreference.

With an increasing number of UEs, the reduction of the actual RF EMF exposure is more significant for EBF and EZF compared to GoB. In the case of EZF, the target is to reduce interference by null-forming, whereas GoB and EBF aim to maximize received power level, which leads to stronger EMF exposure reduction for EZF.

It is important to highlight that the CDF curves, as presented in Figure 10 to Figure 13, can be used as a valid input to the compliance procedure for the installation of BS installation compliance based on the actual maximum EIRP, as described in IEC 62232:2022 [5]. This procedure allows to use CDF obtained from computational modeling to determine the actual maximum EIRP threshold to be used in the RF EMF exposure evaluation. The threshold is identified as a value of CDF corresponding to the given assumed percentile, e.g., 95th percentile. Because the presented CDF curves are normalized to the maximum EIRP and multiplied by the technology duty cycle factor, the identified threshold

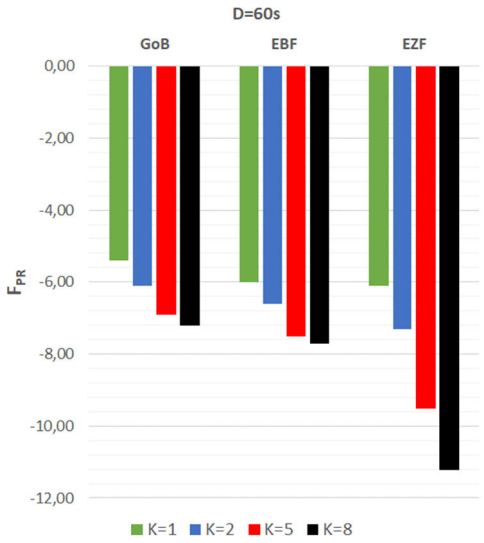

FIGURE 14. Comparison of F_{PR} values for a 95th percentile for different BF schemes in the case of D = 60s, when K = 1, K = 2, K = 5 and K = 8.

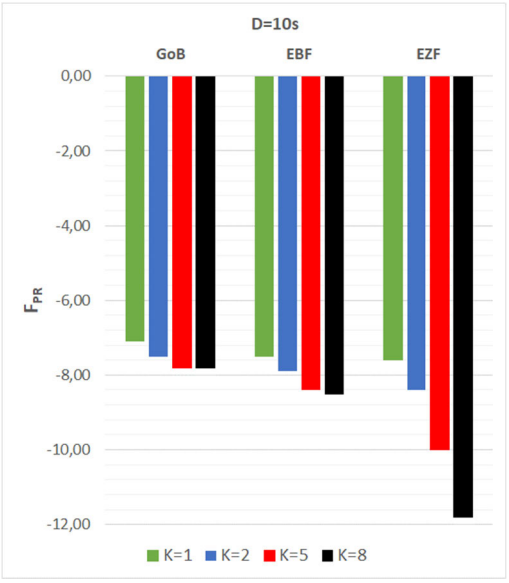

FIGURE 15. Comparison of F_{PR} values for a 95th percentile for different BF schemes in the case of D = 10s, when K = 1, K = 2, K = 5 and K = 8.

corresponds to the F_{PR} as defined in IEC 62232:2022 [5]. The F_{PR} obtained in this way can be used in the actual RF EMF exposure evaluation and configured on the BS to ensure that this threshold, once determined and implemented, is not exceeded during the operation of the BS.

Figure 14 and Figure 15 illustrate change of F_{PR} determined as the 95th percentile of the CDF curves presented in Figures 10 to Figure 13, and Table 2 summarizes its value for the serving time $D = 60$ s. The main observation is that the value of F_{PR} reduces for all BF algorithms when the traffic is more dynamic (more UEs and shorter serving time, that is, higher values of K and lower values of D). When serving time D decreases, the reduction in F_{PR} is stronger for a lower

TABLE 2. FPR values for a 95th percentile for different BF algorithms, number of served UE and serving time of 60 s.

BF scheme	K (-)	D (s)	F_{PR} (-)	F_{PR} (dB)
GoB	1	60	0.31	-5.0
EBF	1	60	0.25	-6.0
EZF	1	60	0.24	-6.1
GoB	2	60	0.26	-5.9
EBF	2	60	0.22	-6.6
EZF	2	60	0.19	-7.3
GoB	5	60	0.20	-6.9
EBF	5	60	0.18	-7.5
EZF	5	60	0.11	-9.5
GoB	8	60	0.19	-7.1
EBF	8	60	0.17	-7.7
EZF	8	60	0.08	-11.2

TABLE 3. Median of normalized EIRP for different BF algorithms.

K [-]	D [s]	GoB	EBF	EZF
		Median of normalized EIRP [dB]		
1	60	-8.6	-9.1	-9.1
2	60	-8.6	-9.1	-9.3
5	60	-8.4	-9.1	-10.3
8	60	-8.3	-9.1	-12.2

number of UEs served, i.e., $K = 1$ and $K = 2$, and this trend is visible for all BF schemes. For example, in the case of GoB the difference between F_{PR} values for $D = 60$ s and $D = 10$ s is 2.1 dB and 1.4 dB for $K = 1$ and $K = 2$, respectively. Whereas, when more UEs are served simultaneously, i.e., $K = 5$ and $K = 8$ this difference is 0.9 and 0.6 dB, respectively. It should be noted that in the case of 5 or 8 UEs in the cell, they are not always served simultaneously using MU-MIMO (separated beams). It depends strongly on their locations in the cell and radio propagation conditions. Pairing many UEs for MU-MIMO is not always possible because inter-beam interference may be too strong and, under these conditions, fewer UEs are paired for MU-MIMO and the remaining UEs are served in different time slots instead of different beams, which is expected to be the main reason of the observed behavior.

Additional interesting observations can be made during the comparison of the median values (50th percentile) of CDF curves in Figure 10 to Figure 13, which are summarized in Table 3 for the serving time $D = 60$ s. As described above, the 95th percentile of normalized EIRP (presented as F_{PR}) evaluated in a certain direction and averaged over 6 minutes decreases with the increase of K or the decreasing of D for all BF schemes. However, in the case of the 50th percentile, the value of normalized EIRP for GoB and EBF does not depend on the number of UEs and serving time. This is because of the conservation of energy, which is independent of the time needed to sum up or average the energy. The

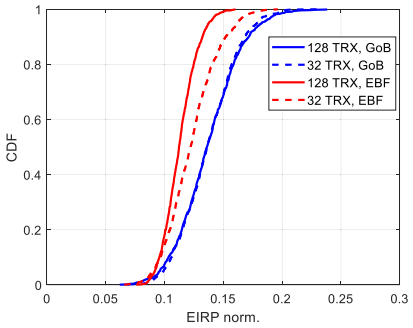

FIGURE 16. CDF of normalized EIRP for mMIMO array with 32 TRX and 128 TRX for GoB and EBF (K = 2, D = 10s).

situation is different in the case of EZF, where the median value of normalized EIRP is reducing when new UE are added. This algorithm reduces energy by beam-nulling and therefore cancelation is stronger when value of K increases. However, when we decrease the serving time D for a given value of K, the median of normalized EIRP does not change also in case of EZF due to energy conservation, as explained above.

B. IMPACT OF ANTENNA ARRAY CONFIGURATION

The previous subsection illustrated that the application of advanced beamforming scheme decreases F_{PR} as compared to GoB and in the case of EBF its value can be lower by 0.5 dB to 1.1 dB (for $D = 60$s). This difference can be even greater when massive MIMO BS is equipped with more TRX, increasing the degrees of freedom in the EBF algorithm. To quantify this difference in the simulation study, the initial number of TRX was increased from 32 to 128 to ensure that every antenna element is connected to separate TRX. Evaluation was carried out for GoB and EBF and one example of CDF with normalized EIRP with $K = 2$ and $D = 10$ s is presented in Figure 16. In the case of GoB, the actual RF EMF exposure is comparable for both antenna array configurations, and the value of F_{PR}, determined as the 95th percentile, increased by 0.1 dB for 128 TRX compared to 32 TRX. This observation is valid under the assumption that for GoB the number and directions of predefined beams are fixed and additional TRX chains do not cause any benefits in terms of performance and EMF reduction. However, a small difference is visible due to better resolution of antenna weights in columns of antenna array for 128 TRX compared to 32 TRX which has 4 antenna elements in one sub-array connected to single TRX per polarization.

The benefits of full digital architecture are more visible when the EBF algorithm is used, which is caused by higher capability of the precoder due to more degree of freedom as compared to the subarray architecture with 32 TRX. This decreases the value of F_{PR} for EBF, which in the case of 128 TRX is 1.2 dB lower than for GoB, whereas it was only 0.4 dB lower in the case of 32 TRX. The results indicate that equipping the BS with more TRX could lower the actual EIRP and decrease EMF exposure beacuse more degree of freedom for BF algorithms results in denser beam resolution and more variance in antenna pattern characteristic (in case of EBF/EZF). To summarize, all the F_{PR} values determined in this study, as well as in [7], have been collected in Table 4. It contains values for different representative configurations, which can be used in RF exposure evaluation of a given BS or configured as an input parameter in the EIRP control algorithm. In this table we excluded cases with D = 360 s because this kind of long continuously serving time for UE is not observed in operational networks. The use cases with D = 10 s and 60 s are more practical but also quite conservative because in operational networks it can be changed even on every subframe. The conservative approach in this case also provides some margin in the practical implementation of the EMF actual maximum approach. As can be seen, the ranges of F_{PR} values are:

- −5.1 dB to −7.8 dB for GoB,
- −6.0 dB to −8.5 dB for EBF,
- −6.1 to −11.8 dB for EZF.

Therefore, it can be concluded that F_{PR} takes the value between −5.1 dB and −11.8 dB, when 1 to 8 UEs are served simultaneously and constantly for 10 s to 60 s using GoB, EBF or EZF beamforming algorithms implemented

TABLE 4. Collection of FPR values obtained from simulation studies performed for 8 × 8 antenna array with different BF algorithms, ues distribution and TRX configurations.

BF scheme	K (-)	D (s)	F_{PR} (dB) for 32 TRX	F_{PR} (dB) for 128 TRX	F_{PR} (dB) for 64 TRX (from [4])
GoB	1	10	-7.0	-6.9	-
		60	-5.1	-5.0	-
EBF		10	-7.5	-8.4	-7.3
		60	-6.0	-7.1	-5.9
EZF		10	-7.6	-	-
		60	-6.1	-	-
GoB	2	10	-7.5	-7.4	-
		60	-6.1	-6.0	-
EBF		10	-7.9	-8.6	-7.6
		60	-6.6	-7.6	-6.5
EZF		10	-8.4	-	-
		60	-7.3	-	-
GoB	5	10	-7.8	-7.7	-
		60	-6.9	-6.8	-
EBF		10	-8.4	-8.9	-7.9
		60	-7.5	-8.3	-7.3
EZF		10	-10.0	-	-
		60	-9.5	-	-
GoB	8	10	-7.8	-7.7	-
		60	-7.2	-7.1	-
EBF		10	-8.5	-9.0	-
		60	-7.7	-8.5	-
EZF		10	-11.8	-	-
		60	-11.2	-	-

in 5G BS array antenna with 32 TRX. This large range of F_{PR} values indicates that careful selection of used value in real BS operation should be underpinned by knowledge about the configuration of base station: antenna array setup, BF schemes and predicted traffic type.

VI. CONCLUSION

This paper has analyzed the impact of different advanced beamforming algorithms and antenna array configurations on the evaluation of the actual RF EMF exposure from massive MIMO BS as specified in IEC 62232:2022 [5]. The analysis is based on the 3D statistical channel modeling tool described in [7], which is expanded to compare GoB, EBF and EZF techniques, as well as antenna arrays with 32 TRX and 128 TRX.

The results of this study indicate that, for advanced beamforming schemes, such as EBF or ZBF, the actual RF EMF exposure is reduced by up to −4 dB in comparison to GoB scheme when 8 UEs are attached to the BS, and, therefore, lower F_{PR} can be considered when implementing the actual maximum approach. Final comparison of the obtained simulation results leads to the conclusion that F_{PR} can take values between −5.1 dB and −11.8 dB, when 1 to 8 UEs are served simultaneously and constantly loaded at full buffer for 10 s to 60 s using GoB, EBF or EZF beamforming algorithms implemented in 5G BS array antenna with 32 TRX. Increasing number of TRX leads to further decreasing value of F_{PR}.

The conclusions shown in the paper are valid also for other frequency bands, size of bandwidth or subcarrier spacings, as values of F_{PR} depend mainly on antenna size, beamforming scheme, deployment type, UE numbers and distribution as well as traffic model.

According to IEC 62232:2022 [5] the F_{PR} values obtained by such computational modeling can be used in RF EMF exposure evaluation and configured in the BS to ensure that EIRP threshold, once determined and implemented, is not exceeded during the operation of the BS. It can be expected that the planned increase of antenna array sizes associated with a higher number of TRX to enable extreme massive MIMO in the forthcoming 5G-advanced and 6G will lead to further reduction of F_{PR} values. This topic is planned to be the subject of the next simulation campaigns, which aim to evaluate F_{PR} values also for 30 minutes of the averaging time as specified in ICNIRP-2020 [4].

ACKNOWLEDGMENT

The authors would like to thank Andreas Weber for his support in system level simulations.

REFERENCES

[1] E. Björnson, L. Sanguinetti, H. Wymeersch, J. Hoydis, and T. L. Marzetta, "Massive MIMO is a reality—What is next? Five promising research directions for antenna arrays," *Digital Signal Process.*, vol. 94, pp. 3–20, Nov. 2019. [Online]. Available: https://www.sciencedirect.com/science/article/pii/S1051200419300776

[2] ICNIRP, "Guidelines for limiting exposure to time-varying electric, magnetic and electromagnetic fields (up to 300 GHz)," *Health Phys.*, vol. 74, pp. 494–522, Oct. 1998.

[3] *IEEE Standard for Safety Levels with Respect to Human Exposure to Electric, Magnetic, and Electromagnetic Fields, 0 Hz to 300 GHz*, IEEE Standard C95.1-2019, 2019.

[4] International Commission on Non-Ionizing Radiation Protection, "Guidelines for limiting exposure to electromagnetic fields (100 kHz to 300 GHz)," *Health Phys.*, vol. 118, no. 5, pp. 483–524, May 2020.

[5] *Determination of RF Field Strength, Power Density and SAR in the Vicinity of Base Stations for the Purpose of Evaluating Human Exposure*, Standard IEC 62232:2022, Oct. 2022.

[6] *Case Studies Supporting IEC 62232—Determination of RF Field Strength, Power Density and SAR in the Vicinity of Radiocommunication Base Stations for the Purpose of Evaluating Human Exposure*, Standard IEC TR 62669:2019, Apr. 2019.

[7] P. Baracca, A. Weber, T. Wild, and C. Grangeat, "A statistical approach for RF exposure compliance boundary assessment in massive MIMO systems," in *Proc. 22nd Int. ITG Workshop Smart Antennas*, Mar. 2018, pp. 1–6.

[8] B. Xu, D. Colombi, P. Joshi, F. Ghasemifard, D. A. Sanjurjo, C. Di Paola, and C. Törnevik, "A summary of actual maximum approach studies on EMF compliance of 5G radio base stations," in *Proc. 16th Eur. Conf. Antennas Propag. (EuCAP)*, Mar. 2022, pp. 1–5.

[9] B. Thors, A. Furuskär, D. Colombi, and C. Törnevik, "Time-averaged realistic maximum power levels for the assessment of radio frequency exposure for 5G radio base stations using massive MIMO," *IEEE Access*, vol. 5, pp. 19711–19719, 2017.

[10] D. Pinchera, M. Migliore, and F. Schettino, "Compliance boundaries of 5G massive MIMO radio base stations: A statistical approach," *IEEE Access*, vol. 8, pp. 182787–182800, 2020.

[11] S. Shikhantsov, A. Thielens, S. Aerts, L. Verloock, G. Torfs, L. Martens, P. Demeester, and W. Joseph, "Ray-tracing-based numerical assessment of the spatiotemporal duty cycle of 5G massive MIMO in an outdoor urban environment," *Appl. Sci.*, vol. 10, no. 21, p. 7631, Oct. 2020.

[12] K. Bechta, C. Grangeat, J. Du, and M. Rybakowski, "Analysis of 5G base station RF EMF exposure evaluation methods in scattering environments," *IEEE Access*, vol. 10, pp. 7196–7206, 2022.

[13] *Study on Channel Model for Frequencies From 0.5 to 100 GHz (Release 15)*, 3GPP, document TR 38.901, 3GPP Radio Access Network Working Group, 2022.

MARCIN RYBAKOWSKI received the M.Sc. degree in electronics and telecommunication (wireless communication) from the Faculty of Electronics, Wroclaw University of Science and Technology, Poland, in 2003, where he is currently pursuing the Ph.D. degree in electromagnetic field exposure for multiantenna systems.

He was with Becker Avionics, Wroclaw, Poland, as an RF Engineer; and Fujitsu, Tokyo, Japan, as an RFIC Engineer. He joined Siemens (then Nokia Siemens Networks), Wroclaw, in 2006, as an Integration and Verification Engineer of 3G and WiMAX Base Stations. He has been a Senior Radio Research Engineer with Nokia Solutions and Networks (then Nokia Bell Labs), since 2012, where he was responsible for research on small cells networks for 3G HSPA systems and radio channel modeling for 5G systems. Since 2016, he has been a Senior Specialist with the Mobile Networks 5G and Small Cell Architecture Department, Nokia, Wroclaw, where he was responsible for specification and architecture of radio modules for 5G systems. Since 2020, he has been responsible for research and development in the area of EMF exposure for massive MIMO systems. He represents Nokia in ETSI as a Delegate for power consumption measurement standards. He is the coauthor of more than 15 articles and ten patents in the area of wireless systems. His research interests include EMF exposure, multiantenna systems, radio wave channel modeling, and evaluation and modeling of wireless systems.

Mr. Rybakowski received the "Young Scientist Award" for the Best Paper presented at the 10th National Symposium of Radio Science (URSI); and the M.Sc. thesis on microwave, antenna, and radar engineering ranked third in a competition organized by the IEEE Polish Section.

KAMIL BECHTA received the M.Sc. and Ph.D. degrees in wireless communications from the Electronics Faculty, Military University of Technology, Warsaw, Poland, in 2010 and 2021, respectively.

After graduation, he was a Research Assistant with the Military University of Technology. In 2011, he joined Nokia Siemens Networks, as a 3GPP RAN4 Standardization Specialist, responsible for RF and RRM requirements of HSPA and LTE. Since 2015, he has been a 5G Senior Radio Research Engineer with Nokia Bell Labs, where he was leading a team responsible for spectrum and co-existence studies for 5G. Since 2017, he has been responsible for specification and RF EMF exposure assessment of radio modules for 5G systems with the Mobile Networks Department, Nokia, Wroclaw, where he has been leading the Research and Development Team, since 2021. Since 2020, he has been representing Nokia in Polish Committee for Standardization, and participates in IEC TC 106 MT 3 Technical Committee for the RF EMF exposure assessment of base stations. He is the coauthor of more than 20 articles and seven patent applications in the area of wireless communications.

Dr. Bechta received the Nokia Technology Center Wroclaw 2nd Award, in 2020; the Foundation for the Development of Radiocommunication and Multimedia Technologies Distinguished Award, in 2022; and the Innovator of Mazovia 1st Award, in 2022.

CHRISTOPHE GRANGEAT received the M.Sc. (Eng.) degree in electronics and microwaves from IMT Atlantique, Université de Bretagne Occidentale, Brest, France, in 1989. He joined Alcatel Research Center, in 1990, where he developed and managed research activity on mobile phone antenna design and RF EMF dosimetry of mobile phones. Since 1990, he has been with Alcatel, Alcatel-Lucent, and Nokia, developed technical expertise in the domain of green telecom, energy efficiency, alternative energies, antenna design, electromagnetic environment, RF exposure dosimetry, and eco-sustainable development of mobile networks. Currently, he is a Principal Architect of mobile networks RAN and an EMF Mitigation Lead with Nokia.

He received the Distinguished Members of Technical Staff (DMTS) Award, in 2014. In 2019, he received the IEC 1906 Award for his contribution to the standardization of RF EMF exposure assessment methods of 5G base stations. He has participated in multiple European and national research programs and has made significant contributions to international standard organizations, such as IEC, CENELEC, ITU, ETSI, and IEEE. Since 2018, he has been a Convenor of the IEC TC106 MT3 Maintenance Team for the RF EMF exposure assessment of base stations (IEC 62232 and IEC TR 62669).

PAWEL KABACIK received the M.Sc. degree (Hons.) in telecommunications and the Ph.D. and D.Sc. degrees in electrical engineering from the Wroclaw University of Science and Technology, Poland, in 1986, 1996, and 2006, respectively. In January 1987, he joined the Institute of Telecommunications and Acoustics, Wroclaw University of Science and Technology, where he is currently an Associate Professor. He was a Visiting Scholar with the Technical University of Denmark (1991–1992), and the University of Queensland, Australia (1997, 2001, and 2006). He chaired the Mulitband Antennas and Conformal Array Mini-Team within the COST 260 Project. Currently, he chairs one of the four research tasks in the COST 284 Project. He plays the role of expert with the European Commission. He has been a Principal Investigator on several research projects funded by the National Research Council of Poland, and national and international companies. His research interests include highly integrated and lightweight antenna arrays, conformal antennas, terminal antennas, phased arrays, advanced antenna measurements, and communication subsystems of small spacecraft. In 1993, he received the Young Scientist Award at the 7th National DRSI Symposium, Poland. In 2000, he received the Harold A. Wheeler Applications Prize Paper Award, Honorable Mention. He was a recipient of the 2007 Pro-Student Award from the Student Self-Autonomy Association of universities and other tertiary institutions in the city of Wroclaw. His name is listed in seven editions of Marquis's Who's Who in Science and Engineering.